ELSEVIER

Journal of Organometallic Chemistry 544 (1997) 163–174

Journal of Organometallic Chemistry

Single component N–O chelated arylnickel(II) complexes as ethene polymerisation and CO/ethene copolymerisation catalysts. Examples of ligand induced changes to the reaction pathway

Sylvie Y. Desjardins [a], Kingsley J. Cavell [a,*], Jason L. Hoare [a], Brian W. Skelton [b], Alexander N. Sobolev [b,1], Allan H. White [b], Wilhelm Keim [c]

[a] *Department of Chemistry, University of Tasmania, GPO Box 252C, Hobart, Tas. 7001, Australia*
[b] *Department of Chemistry, University of Western Australia, Nedlands, W.A. 6907, Australia*
[c] *Institut für Technische Chemie und Petrolchemie der RWTH Aachen, Templergraben 55, D-52056 Aachen, Germany*

Received 5 November 1996

Abstract

Arylnickel(II) phosphine complexes containing substituted N–O bidentate ligands, of the type [NiR(N–O)L] [N–O = 4-nitropyridine-2-carboxylate (4-NO_2-pyca), R = *o*-tolyl, L = PPh_3; N–O = 2-pyrazinecarboxylate (pyzca), R = *o*-tolyl, L = PPh_3; and N–O = 4-methoxypyridine-2-carboxylate (4-MeO-pyca), R = *o*-tolyl, L = PPh_3] have been prepared and characterised. Single crystal X-ray studies of the complexes [Ni(*o*-tolyl)(pyca)PPh_3], **1**, and the isomorphous analogue [Ni(*o*-tolyl)(4-NO_2-pyca)PPh_3], **3**, show the expected square planar coordination about the nickel centres, with the pyridine nitrogens being *trans* to the phosphine ligand for both compounds. The coordination spheres of the two complexes are very similar, no elongation of the Ni–N bond for complex **3**, which contains the 4-NO_2-pyca ligand, being evident. In complex **3** the *o*-tolyl ligand is disordered over two sites indicating the presence, in the solid state, of two conformers in which the *o*-methyl groups of *o*-tolyl are located to either side of the coordination plane. The complexes with substituted pyca ligands form single component catalysts for the conversion of ethene to high molecular weight polyethene and for the copolymerisation of ethene and carbon monoxide to polyketone under mild conditions. The nature of the product, whether predominantly high molecular weight polymer or a mixture of polymer and lower oligomer, is dependent on the basicity of the N–O chelate ligand. From an NMR study of the effect of added ethene on the complex [Ni(*o*-tolyl)(4-NO_2-pyca)PPh_3], a mechanism involving alkene promoted ligand dissociation is suggested. © 1997 Elsevier Science S.A.

Keywords: Arylnickel complexes; X-ray structures; Polymerisation; Copolymerisation; Ethene; Carbon monoxide

1. Introduction

In the study of migratory insertion into d^8 metal–carbon bonds, partial dissociation of the chelate ligand has been proposed as a reaction pathway in some cases [1,2]. In instances where the chelate is either too rigid or too firmly bound, initial dissociation of an alternative weakly bound monodentate ligand (e.g. PPh_3, CH_3CN, halide) possibly occurs [3–7].

Recently, the CO and alkene insertion/deinsertion behaviour of square planar hydrocarbyl complexes of palladium(II) and platinum(II) containing N–O bidentate ligand derived from pyridinecarboxylate (pyca) has been investigated in detail by our group [4,5,8,9]. It was shown that the insertion of CO into the metal carbon bond was facile and that modifications to the pyca ligand could cause changes in the CO insertion pathway and insertion rate. For complexes containing a weakly bound phosphine ligand (e.g. [PtMe(pyca)PPh_3]) an insertion mechanism involving initial phosphine dissociation followed by CO coordination and partial chelate displacement was proposed [5]. For complexes containing strongly bound, highly basic phosphine ligand (e.g. PCy_3), CO insertion is precluded unless the hemilability of the bidentate ligand is electronically or sterically enhanced. The introduction of a nitro substituent in the pyridyl ring of the pyca ligand was shown to weaken the M–N bond and promote an insertion pathway possi-

* Corresponding author.

[1] On leave from L. Karpov Institute of Physical Chemistry, Vorontsova Pole 10, Moscow 103064, Russia.

PII S0022-328X(96)06953-7

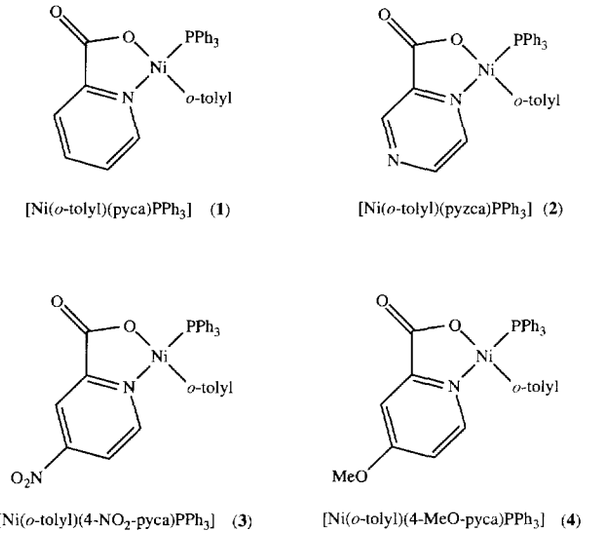

[Ni(*o*-tolyl)(pyca)PPh_3] (**1**) [Ni(*o*-tolyl)(pyzca)PPh_3] (**2**)

[Ni(*o*-tolyl)(4-NO_2-pyca)PPh_3] (**3**) [Ni(*o*-tolyl)(4-MeO-pyca)PPh_3] (**4**)

Fig. 1. Numbering scheme for the complexes [NiR(N–O)L].

bly via initial partial chelate displacement [9]. These neutral complexes did not show any catalytic activity for CO and/or ethene conversion. However, replacement of anionic pyca in the Pd(II) complexes by the neutral ester or amide of pyca provided cationic complexes, which are catalytically active for CO/ethene copolymerisation [10].

Subsequent to our modelling studies on the hydrocarbyl Pd(II) and Pt(II) complexes containing the pyca ligand, we described the use of analogous nickel(II) complexes in catalysis. We were able to demonstrate that arylnickel(II) complexes (Fig. 1, complex **1**) form single component catalysts for the oligomerisation of ethene [11].

It is generally more common for nickel complexes to dimerise or oligomerise lower olefins rather than catalyse the formation of high molecular weight polymer [12]. Moreover, the use of nickel complexes as CO/ethene copolymerisation catalysts has not been widely investigated and only a few examples have been reported [13–16]. A major problem is the facile formation of nickel tetracarbonyl. In this paper we describe the preparation and characterisation of three new nickel(II) complexes of type [NiR(N–O)L] containing substituted N–O pyca ligands (Fig. 1). These new complexes form single component catalysts for the formation of polyethylene from ethene and for the formation of polyketone from ethene and carbon monoxide. Complexes containing pyca with an electron withdrawing nitro group [N–O = 4-nitro-2-pyridinecarboxylate (4-NO_2-pyca), R = *o*-tolyl, L = PPh_3] and a weak donor group [N–O = 4-methoxy-2-pyridinecarboxylate (4-MeO-pyca), R = *o*-tolyl, L = PPh_3 (**3**)] have been prepared and catalytically tested. We have also investigated the effects of including a further heteroatom (N) in the ring [N–O = 2-pyrazinecarboxylate (pyzca), R = *o*-tolyl, L = PPh_3 (**2**)]. A single crystal X-ray study of the complex [Ni(*o*-tolyl)(4-NO_2-pyca)PPh_3] is also reported herein. The structure of the isomorphous complex [Ni(*o*-tolyl)(pyca)PPh_3] has also been obtained for comparison. The new complexes, containing substituted pyca chelate ligands, demonstrate the effect on catalysis of electronic modifications to the N–O ligand.

2. Experimental

All experimental manipulations were carried out under an inert oxygen free dry nitrogen atmosphere using standard vacuum-line and Schlenck techniques unless otherwise stated [17]. Solvents were dried and purified by standard methods and freshly distilled before use [18]. Other reagents were used as received. Complexes $[NiX_2L_2]$ [19,20] and $[NiRXL_2]$ [11] were prepared according to previously published procedures. CP grade ethene and carbon monoxide were obtained from Matheson Gases.

Nuclear magnetic resonance (NMR) spectra were recorded at room temperature (20 °C) (unless otherwise indicated) on a Brüker AM-300 NMR spectrometer at 300.13 MHz (^{1}H) and 121.50 MHz (^{31}P). Solutions were prepared in deuterated benzene. Chemical shifts (δ) are reported in ppm relative to internal $SiMe_4$ (^{1}H), or to external 85% H_3PO_4 (^{31}P). Coupling constants (J) are given in Hz. NMR peaks are given as singlet (s), doublet (d), triplet (t) and multiplet (m).

Infrared (IR) spectra were recorded on a Hitachi 270-30 IR spectrophotometer, and a Brüker IFS-66 FTIR spectrometer. Potassium bromide disks were used in the mid IR range (4000–400 cm^{-1}). Absorption frequencies (cm^{-1}) are described as very strong (vs), strong (s), medium (m) or weak (w) in intensity.

Microanalyses were carried out on a Carlo Erba CHNS-O EA1108 elemental analyser by the Central Science Laboratory (CSL), University of Tasmania.

Mass spectra were obtained, using the methane desorption chemical ionisation method, on a Kratos Concept ISQ mass spectrometer by the CSL.

2.1. Structure determinations

Unique diffractometer data sets ($T \sim 295$ K; monochromatic Mo Kα radiation, $\lambda = 0.7107_3$ Å; $2\theta/\theta$ scan mode; $2\theta_{max} = 50°$) were measured yielding N independent reflections, N_o with $I > 3\sigma(I)$ being considered 'observed' and used in the full matrix least squares refinements after Gaussian absorption correction. Anisotropic thermal parameters were refined for the non-hydrogen atoms, $(x, y, z, U_{iso})_H$ being con-

strained at estimated values. Conventional residuals on $|F|$ at convergence R, R_w are quoted; statistical weights were derivative of $\sigma^2(I) = \sigma^2(I_{diff}) + 0.0004\sigma^4(I_{diff})$. Neutral atom complex scattering factors were employed, computation using the XTAL 3.2 program system implemented by S.R. Hall [21]. Pertinent results are given in the figures and tables; material deposited comprises structure factor amplitudes, thermal and hydrogen atom parameters and full molecular geometry.

2.1.1. Crystal / refinement data

[Ni(*o*-tolyl)(pyca)PPh_3]**1** = $C_{31}H_{26}NNiO_2P \cdot 5/6$thf, $M = 594.2$, rhombohedral space group $R\bar{3}$ (C_{3i}^2, No. 148) (hexagonal setting); $a = 31.485(7)$, $c = 15.677(3)$ Å, $V = 13459$ Å^3, $D_C(Z = 18) = 1.32$ g cm^{-3}; $F(000) = 5604$; $\mu_{Mo} = 7.3$ cm^{-1}; specimen: irregular ≈ 0.3 mm; $A^*_{min,max} = 1.42$, 1.60; $N = 5249$, $N_o = 3250$; $R = 0.049$, $R' = 0.056$; $n_v = 387$.

[Ni(*o*-tolyl)(4-NO_2-pyca)PPh_3]**3** = $C_{31}H_{25}N_2NiO_4P \cdot 5/6$thf, $M = 639.2$, space group $R\bar{3}$; $a = 32.160(9)$, $c = 16.048(2)$ Å, $V = 14373$ Å^3, $D_C(Z = 18) = 1.33$ g cm^{-3}; $F(000) = 6000$; $\mu_{Mo} = 6.9$ cm^{-1}; specimen: $0.53 \times 0.32 \times 0.26$ mm^3; $A^*_{min,max} = 1.14$, 1.17 (Gaussian); $N = 5429$, $N_o = 4955$; $R = 0.083$, $R' = 0.058$; $n_v = 478$.

The two complexes are isomorphous and were refined in the same cell and coordinate setting. Difference map residues were modelled in terms of thf solvent molecules of two types, one (unprimed) disordered about the set of three axes (Wyckoff *a*) passing through (0,0,0), site occupancy 1/3, the other (primed) disordered about the inversion centres derivative of (1/2,1/2,1/2) (Wyckoff *d*), site occupancy 0.5, the former lying in a conspicuous tunnel in the lattice parallel to *c*. No disorder is found in the complex molecule in the pyca complex, but in its 4-NO_2-pyca analogue, the *o*-tolyl group, which lies normal to the coordination plane, and which, in the pyca adduct, has its 2-methyl substituent lying close to one of the disordered thf moieties (Wyckoff *d*), is here rotationally disordered about the C(1)–C(4) ring axis, the displacement of the group being such that individual components are resolvable for all non-hydrogen atoms and refinable with anisotropic thermal parameter forms; site occupancies were set at 0.5 after trial refinement, possibly concerted with those of the nearby thf. The inherently lower precision of the determination, reflected in higher R (but only slightly higher R_w), consequent upon the presence of the disorder, is offset to a considerable extent by the accessibility of more extensive data from a larger available specimen, and results of useful precision are obtained in respect of the metal atom environment, although caution is needed in their use, particularly those pertaining to the disordered *o*-tolyl group, where the coordinated atom components are resolvable.

2.2. Synthesis of 4-NO_2-pyca and 4-MeO-pyca

The substituted pyridine carboxylate ligands used in this work were prepared according to procedures adapted from the methods of Krohnke and Schafer [22], Matsumura et al. [23] and Brown and Shambu [24].

2.2.1. 4-Nitropyridine-N-oxide

Pyridine-N-oxide (16.76 g, 0.176 mol) was dissolved with stirring in concentrated sulphuric acid (53 ml) at 0 °C. A mixture of concentrated nitric acid (63 ml) and concentrated sulphuric acid (53 ml) was added slowly. The reaction mixture was heated at 160 °C for about 2 h, until NO_2 evolution had ceased. The pH was adjusted to around 7.5 with approximately 10 M NaOH solution, with initial cooling followed by gentle heating to prevent inorganic salt precipitation. During this neutralization the yellow/orange product precipitated and was collected by filtration. The product was recrystallized from chloroform and dried in vacuo. Yield 48%. ^{1}H NMR (DMSO-d_6): δ 8.42m and 8.21m (4H, J = 7.74 Hz).

2.2.2. 2-Cyano-4-nitropyridine

The preparation and storage of this compound were performed in an atmosphere of nitrogen. 4-Nitropyridine-N-oxide (9.58 g, 0.068 mol) and dimethylsulphate (7 ml, 0.07 mol) were placed in a two-neck round bottom flask equipped with a magnetic stirring bar, nitrogen inlet and reflux condenser. The mixture was heated at 65–70 °C with stirring for 2 h. Upon cooling a salt crystallized and was dissolved in 25 ml water. The reflux condenser was replaced by a dropping funnel, and a solution of potassium cyanide (5.2 g in 20 ml water) was added dropwise with vigorous stirring, at −7 to −8 °C. After standing overnight the precipitate was collected by filtration. Yield 73%. ^{1}H NMR ($CDCl_3$): δ 9.08 (d, J = 5.2 Hz, 1H), 8.44 (d, J = 3.3 Hz, 1H) and 8.29 (m, 1H).

2.2.3. 4-Nitropicolinic acid

A solution of 2-cyano-4-nitropyridine (3.82 g, 0.026 mol) in 40 g of 90% sulphuric acid was heated at 120 °C for 2 h. Into the reaction mixture, at 20–25 °C, was added dropwise with stirring a solution of sodium nitrite (5 g in 10 ml water). The mixture was stirred at 20–25 °C for a further hour, then at 80 °C for 1 h. The resulting solution was poured onto 50 g of cracked ice and neutralized with solid sodium carbonate to pH 1.6. The resulting pale brown/yellow product was collected via filtration and dried in vacuo. Yield 89%. ^{1}H NMR (DMSO-d_6): δ 9.09 (d, J = 5.2 Hz, 1H), 8.53 (d, J = 2.2 Hz, 1H), 8.37 (m, 1H). The acidic proton was not observed due to rapid exchange with trace moisture in

the solvent. FTIR: 1698.7s and 1308.1s [ν(O–C=O)]; 1540.5s and 1357.2s [ν(O–N=O)]; 845.6m [ν(C–N)].

2.2.4. 4-Methoxypicolinic acid

4-Nitropicolinic acid (2.5 g, 0.0149 mol) was added slowly to a solution of 1.6 g (0.07 mol) sodium in 75 ml dry methanol and refluxed under nitrogen for 2 h. The methanol was removed by distillation, and the residue was neutralized to around pH 3 with HCl. An excess of saturated copper sulphate solution was added to the mixture to precipitate the methoxy acid as the copper salt. The free acid was obtained by suspending the copper salt in hot water, and passing hydrogen sulphide gas through the suspension. The solution was filtered, the solvent removed by rotary evaporation, and the solid recrystallized from ethanol. The product was obtained as a white solid in 90% yield. ^{1}H NMR (DMSO-d_6): δ 8.68 (d, J = 5.80 Hz, 1H), 7.77s, 7.55 (d, J = 3.60 Hz, 1H), 4.07 (s, 3H, CH_3O-py, 3H). The acidic proton was not observed due to rapid exchange with trace moisture in the solvent. FTIR: 1736.7s and 1307.8s [ν(O–C=O)], 1408.9m [C–O–H bend], 1226.0s and 1016.3m [ν(C–O–C)].

2.3. Synthesis of the ligand salts Tl(4-NO_2-pyca), Na(4-MeO-pyca) and Tl(pyzca)

The ligands Tl(4-NO_2-pyca), Na(4-MeO-pyca) and Tl(pyzca) were prepared using the same procedure previously published for Tl(pyca) and Na(pyac) [11].

2.3.1. Thallium(pyca)

White powder. ^{1}H NMR (CD_3OD): δ 9.27 (s, 1H, H3), 8.82 (m, 1H, H6), 8.75 (m, 1H, H5). FTIR: 1614.4s [ν(C=O)], 1592s, 1567m [ν(C=C), (C=N)].

2.3.2. Thallium(4-NO_2-pyca)

Yellow powder. FTIR: 1622.3s [ν(C=O)], 1600s, 1562m [ν(C=C), (C=N)], 1534.9s [ν_a(O–N=O)], 1553.8 [ν_s(O–N=O)]. MS: m/z MH^+ 373, 358, 222, 205.

2.3.3. Sodium(4-MeO-pyca)

Dark grey powder. ^{1}H NMR (DMSO-d_6): δ 3.84 (s, 3H, CH_3–O–), 6.9 (m, 1H, H5), 7.53 (d, 1H, H3), 8.28 (d, 1H, H6). IR: 1610s [ν_s(C=O)], 1583s, 1563s [ν(C=C) or (C=N)].

2.4. Synthesis of the complexes [Ni(o-tolyl)(N–O)PPh_3]

The synthesis of [Ni(o-tolyl)(pyca)PPh_3] has been reported previously [11]. The complexes [Ni(o-tolyl)(pyzca)PPh_3] (**2**), [Ni(o-tolyl)(4-NO_2-pyca)PPh_3] (**3**) and [Ni(o-tolyl)(4-MeO-pyca)PPh_3] (**4**) were also prepared according to the previously published procedures [11], the only difference being that the complexes typically required a longer reflux period (2–4 h) to drive the reaction to completion. For complex [Ni(o-tolyl)(4-NO_2-pyca)PPh_3] (**3**), precipitated TlBr was removed by centrifugation following filtration through Celite. Characterisation details for the complexes (**2–4**) are given below.

2.4.1. Ni(o-tolyl)(pyzca)PPh_3 (2)

Yield 85%; yellow crystalline powder. ^{1}H{^{31}P} NMR (C_6D_6): δ 2.50 (s, 3H, o-$CH_3C_6H_4$), 6.49 (m, 1H, H5), 7.35 (d, 1H, o-H), 7.45 (s, 1H, H6), 9.27 (s, 1H, H3), {24.96, PPh_3}. IR: 3050w, 2955w, 1670vs, 1600w, 1583w, 1490w, 1480w, 1433w, 1410w, 1337m, 1173w, 1097m, 1048w, 855w, 795w, 743m, 693m, 533m, 506m, 465m. MS: m/z MH^+ 536, 353, 333, 279, 263. Anal. Found: C, 66.99; H, 4.88; N, 5.10. Calc.: C, 67.33; H, 4.71; N, 5.23%.

2.4.2. Ni(o-tolyl)(4-NO_2-pyca)PPh_3 (3)

Yield 86%; deep red crystals. ^{1}H{^{31}P} NMR (C_6D_6): δ 2.61 (s, 3H, o-$(CH_3)C_6H_4$), 6.40 (dd, 1H, H5), 6.7 (H6), 7.35 (s, 1H, o-H), 8.32 (s, 1H, H3), {24.26, PPh_3}. IR: 3044w, 2968w, 1672vs, 1606w, 1572w, 1538s, 1482m, 1436s, 1348s, 1324s, 1245m, 1180m, 1096m, 1068m, 909w, 835w, 744s, 694s, 532s, 506m, 464w, 442w, 414w. Anal. Found: C, 64.65; H, 4.96; N, 4.43. Calc.: C, 64.54; H, 5.11; N, 4.30%.

2.4.3. Ni(o-tolyl)(4-MeO-pyca)PPh_3 (4)

Yield 81%; light yellow crystalline powder, ^{1}H{^{31}P} NMR (C_6D_6): δ 2.63 (s, 3H, OCH_3), 2.70 (s, 3H, o-$(CH_3)C_6H_4$), 5.75 (dd, 1H, H5), 6.75 (H6), 7.49 (s, 1H, o-H), 7.55 (s, 1H, H3), {26.51, PPh_3}. IR: 1665s, 1614m, 1560w, 1481m, 1454w, 1433m, 1331s, 1304w, 1250w, 1094m, 1037m, 902w, 829w, 806m, 740m, 694s, 535w, 515m, 493w. Anal. Found: C, 68.36; H, 5.07; N, 2.42. Calc.: C, 68.12; H, 5.00; N, 2.48%.

2.5. Catalytic testing

Catalytic testing was carried out at 40–55 bar in a medium pressure 75 ml stainless steel autoclave equipped with magnetic stirring bar, a manometer, two gas valves and fitted with a glass liner. The autoclave was magnetically stirred and heated to 80 °C over the reaction period (12 h) in an oil bath controlled by a thermocouple.

2.5.1. Ethene polymerisation

Typically, the autoclave was assembled hot then evacuated and flushed three times with dry nitrogen. An aliquot, containing between 0.06 and 0.1 mmol of the [NiR(N–O)L] complex in 10–15 ml toluene, was transferred under nitrogen from a standard solution to the autoclave with a gas tight syringe. The autoclave was pressurised with ethene to 40 bar at room temperature and then placed in an oil bath, preheated to the required

temperature (generally 80 °C). Stirring was started and thermal equilibrium was reached within approximately 15 min and the reaction was timed from then. The autoclave containing the reagents was weighed before and after a catalytic run to ensure no leakage of ethene had occurred. After the reaction time (12 h) the autoclave was cooled to approximately −10 °C in an ice/salt bath and carefully depressurised while stirring. Nonane (0.1 ml) was added as an internal standard prior to GC analysis of the products.

2.5.2. Carbon monoxide and ethene copolymerisation

Copolymerisation experiments required the catalyst to first be activated in the presence of ethene only. The autoclave was pressurised with ethene to 40 bar at room temperature. After the pressure was stabilised, the autoclave was then pressurised with an additional 2–5 bar of carbon monoxide (0.1–0.6 g) to a total pressure of 42–45 bar while stirring. From that point, the experimental method was the same as that described for ethene polymerisation.

2.6. Product analysis

Gas chromatographic analyses were carried out on the final products by injecting a 0.3 μl sample into a HP 5890 GC fitted with an SGE QC3/BP1-1.0 or SGE QC3/BP1-2.0 capillary column using N_2 as carrier gas, a flame ionisation detector (FID) and a split/splitless sample injector. Integration was performed using DAPA software. Peak assignment had previously been carried out [25,26].

The initial oven temperature was 35 °C with a ramp rate of 10 °C min^{-1} and a head pressure of 100–150 KPa. When present, olefin oligomers were identified by GC-MS. C_6 olefin isomers used to determine linearity and percentage of alpha olefins were separated from the crude sample by distillation and individually resolved on a Siemans Sichromat 3 using a 50 m PONA FS HP capillary column. Separation of the isomers was achieved with an initial oven temperature of 30 °C, an isothermal time of 20 min followed by a ramp rate of 20 °C min^{-1}.

The polymeric material was recovered by filtration and stirred in methanol/HCl solution to remove traces of nickel compounds, filtered, washed with aliquots of methanol and dried in air. The molecular weight range of selected samples of polyethylene was determined by ICI Australia Operation Pty Ltd.

The catalytic activity is quantified by the turnover number (TON) expressed as [total mole of substrate consumed/mole nickel complex used]. The TON takes into account the total amount of products formed (liquid oligomers and polymers (polyethylene or polyketone)). The amount of polymer produced is quantified by the percentage of polymer formed with respect to the total product and is expressed as %PE (per cent polyethylene) and %PK (per cent polyketone) in the relevant sections.

3. Results and discussion

3.1. Preparation and characterisation of the complexes

The nickel(II) complexes were prepared in high yield (80–90%) by the reaction of sodium or thallium salts of the anionic (N–O) ligands with nickel(II) *trans*-$NiX(R)(L)_2$ at room temperature in tetrahydrofuran [11].

The synthesis of nickel(II) complexes [NiR(N–O)L] discussed in this work involves displacement of one monodentate phosphine ligand by the incoming chelate. The formation of TlX by halide abstraction helps drive the reaction to the desired product; use of the sodium salts of the ligands required more severe conditions. The complexes are air stable in the solid state. In solution, they are stable for several days in dry solvents under an inert atmosphere. The complexes are readily soluble in a range of solvents but insoluble in hydrocarbon solvents (hexane, heptane) and they decompose in chlorinated solvents.

^{1}H NMR spectra of the nickel complexes indicate the formation of only one isomer in solution. The preferred isomer has the pyridine nitrogen *trans* to the phosphine, as confirmed by the X-ray studies.

The presence of the nitro and methoxy substituents in the 4-position of the pyridyl ligands leads to a very large deshielding effect on proton H3 (Table 1). In complex **3**, where the 4-pyridyl position is occupied by the nitro substituent, proton H3 resonates at δ 8.32 ppm, a shift of 1.42 ppm downfield relative to H3 in complex **1**, which occurs at 6.90 ppm. In complex **4**, where the 4-pyridyl position is occupied by the mildly electron donating methoxy substituent, proton H3 resonates at δ 7.55 ppm with a shift of 0.65 ppm with respect to **1**. This is consistent with the expected downfield shift of protons adjacent to *para*-substituents of increasing electron attracting power [27]. Proton H3 is further deshielded by the presence of an *ortho* nitrogen atom in the 4-position for complexes containing pyrazyl ligands [**2**, δ 9.27 ppm; $\Delta\delta = 2.37$ ppm with respect to **1** (Table 1)]. For complex **4**, the chemical shifts of the *o*-Me protons on the *o*-tolyl ligand (δ 2.70 ppm) and the –OMe protons on the pyridine ligand (δ 2.82 ppm) which resonate in the same area were assigned unambiguously on the basis of long range coupling observed in the COSY spectrum of **4**.

All complexes exhibited characteristic strong bands in their IR spectra in the region 1665–1672 cm^{-1}, which are assigned to (C=O) stretching vibrations. Selected IR data are listed in Table 1.

Semi-empirical PM3 calculations were performed on

Table 1
Selected ^{1}H NMR and IR data for Ni(II) complexes of the type [NiR(X-pyca)L]

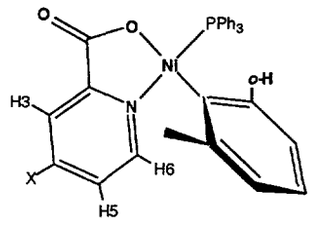

Complex	^{1}H NMR (in benzene-d_6) (ppm)				IR (in KBr) (cm^{-1})		
	o-Tolyl group		Pyridyl ring		ν(C=N)	ν(C–O)	ν(C=O)
	o-Me	*o*-H	H3	C–X			
2	2.50s	7.35d J_{HH} = 7.6 Hz	9.27d J_{HH} = 2.4 Hz	N	1600	1337	1670
3	2.61s	7.35d J_{HH} = 7.2 Hz	8.32d J_{HH} = 2.4 Hz	C–NO_2	1606	1324	1672
4	2.70s	7.49d J_{HH} = 7.3 Hz	7.55d J_{HH} = 1.8 Hz	C–OCH_3 2.82s	1614	1331	1665

the free N–O ligands used in this work, employing MOPAC93. Geometries were fully optimised and Mulliken population analyses employed to investigate substituent effects on the electron distribution, one of the important properties influencing base strength (Table 2) [28]. It is apparent from the calculations that, with respect to the non-substituted pyridyl ligand (pyca), the electron withdrawing *para*-nitro substituent significantly reduces the effective charge density on the nitrogen atom, while the mildly electron donating *para*-methoxy group increases the charge density. The relative basicities of the bidentate N–O ligands vary in the order 4-MeO-pyca > pyca > pyzca > 4-NO_2-pyca.

3.2. Catalytic results

Analogous complexes of the type [Ni(*o*-tolyl)(pyca)L] (where L = monodentate tertiary phosphine and pyca = 2-pyridinecarboxylate) were found to form moderately active single component ethene oligomerisation catalysts producing mainly linear olefins (96–98%) containing between 40 and 85% α-olefins depending on the nature of the phosphine ligand [11]. In palladium(II) complexes it had been noted that the presence of a substituent on the pyridyl ring of the chelate ligand led to a modification in the CO insertion pathway [9]. Therefore, it was felt that a similar variation in the N–O chelate ligand may influence the catalytic behaviour of nickel(II) catalysts containing these ligands. Consistent with this expectation it was observed that under the same catalytic conditions, complexes containing 4-substituted pyca ligands form single component catalysts for the polymerisation of ethene and for the copolymerisation of CO and ethene.

Table 2
Semi-empirical determination of absolute charge on the pyridyl nitrogen atom in N–O ligands

Ligand	Absolute charge on nitrogen
pyca	−0.0639
pyzca	−0.0256
4-NO_2-pyca	−0.0140
4-MeO-pyca	−0.1008

Catalytic performances for ethene homopolymerisation and CO/ethene copolymerisation, reported in Table 3, indicate that the activity and the percentage of polymer in the product varies with the basicity of the N–O chelate ligand. For ethene homopolymerisation complex **3**, [Ni(*o*-tolyl)(4-NO_2-pyca)PPh_3], forms the most active catalyst (activities of up to 225 g PE g^{-1} Ni h^{-1} were obtained) and products consist of 90–100% high density, high molecular weight polyethene (T_m = 129.5 °C). Very small amounts of liquid oligomers were also produced. For complex **2**, [Ni(*o*-tolyl)(pyzca)PPh_3], the product distribution consisted of a mixture of oligomers and polyethene, with approximately 55% of the product being polyethene. The oligomer fraction was highly linear (~ 99%). However, considerable isomerisation occurred and only 66% was α-olefin. The catalyst derived from complex **4**, [Ni(*o*-tolyl)(4-MeO-pyca)PPh_3], showed the lowest TON (500 ± 100). Interestingly, the product distribution obtained from complex **4** is similar to that for catalysts containing non-substituted pyca ligands [11], and contains mainly liquid oligomers with small amounts of polyethene (10–20%), indicating that the rates of propagation and termination are similar for this catalyst. The liquid oligomeric products obtained displayed a typical Schulz–Flory distribution of chain lengths, supporting the concept of a single stepwise chain growth mechanism.

Table 3
Catalytic results for ethene polymerisation and CO/ethene copolymerisation with nickel complexes of the type [Ni(*o*-tolyl)(X-pyca)PPh_3]

Complex	C_2H_4				C_2H_4/CO	
	TON	PE (%)	Linear olefins [a] (%)	Linear α-olefins [a] (%)	TON	PK %
2	800	55	98	77	50	~ 70
3	1700	80–100	89	79	170	~ 100
4	500	10–20	97	56	360	~ 10–20

Reaction conditions. Ethene only; 0.5–0.6 mmol complex in toluene solvent, 80 °C, ethene pressure 40 bar, reaction time 12 h. CO/ethene; 40 bar ethene and 2–5 bar CO.
[a] Determined from the C6 fraction.

Few examples of fully characterised nickel(II) complexes that are active for CO/C_2H_4 copolymerisation have been reported [13–16]. However, systems based on modified SHOP-type nickel complexes have been shown to copolymerise CO and C_2H_4 to high molecular weight polyketone [13–15]. The unusual feature of the nickel based copolymerisation systems is that they must be initiated in the absence of CO which acts as a poison. Hence the active intermediate is generated in the presence of ethene only, as is the case for homopolymerisation. GC-MS analysis of the initial reaction products confirmed the presence of 2-methylstyrene, generated from initial ethene insertion. On the addition of CO, products formed from that point incorporated CO, resulting in the production of perfectly alternating CO/C_2H_4 copolymer (Fig. 2). Carbon monoxide concentration is a critical factor in the production of polyketone and only a very narrow window of CO concentration resulted in active catalysts. CO pressure above 5 bar completely deactivated the catalyst and at CO pressures below 2 bar no activity for copolymerisation was observed.

The catalyst derived from complex **3**, [Ni(*o*-tolyl)(4-NO_2-pyca)PPh_3], selectively copolymerises CO and C_2H_4 to high molecular weight polyketone ($T_m \approx$ 240 °C). Microanalysis and infrared data for the polymer shows perfectly alternating polyketone. GC analysis of the liquid fraction shows the presence of only trace amounts of dimers and trimers of ethene. No higher ethene oligomers or oligomeric keto products were detected. The catalytic activity for copolymerisation is low with respect to the homopolymerisation

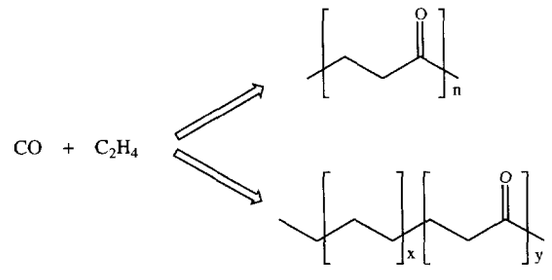

Fig. 2. Types of polymer formed in the CO/ethene copolymerisation reaction.

activity (Table 3), as has previously been noted [13]. Complex **2**, [Ni(*o*-tolyl)(pyzca)PPh_3], yielded a product consisting of approximately 70% polyketone, the rest being primarily oligomeric species. Infrared and elemental analysis of the product also suggested the presence of block copolymer (Fig. 2). In addition, GC analysis of the remaining liquid fraction revealed that it consisted mainly of ethene oligomers. The catalyst derived from complex **4**, [Ni(*o*-tolyl)(4-MeO-pyca)PPh_3], produced mainly ethene oligomers, the copolymer constituting only 10–20% of the total products. The substantial proportion of ethene oligomers produced with complexes **2** (30%) and **4** (80–90%) would seem to suggest that oligomerisation continues even after the addition of CO. Why this occurs is not entirely clear, considering that CO (being a better π acid) has a greater affinity for the metal centre [29].

The presence of excess phosphine, or highly basic phosphine ligands (e.g. PCy_3), has been shown to completely suppress carbonylation [5,30,31] and copolymerisation [32]. This is presumably due to the phosphine blocking coordination sites, preventing the coordination of substrate. Consistent with these previous observations, catalytic testing of complex **3** in the presence of one equivalent of free triphenylphosphine, under standard conditions, resulted in complete deactivation of the system. Importantly, this is in contrast to our previous observations for Ni(pyca) complexes during ethene oligomerisation [11], and possibly indicates that different insertion pathways are being followed for the two sets of catalysts.

Attempts to isolate a nickel aroyl complex were unsuccessful. However, migratory insertion of CO could be followed by ^1H NMR. Carbon monoxide was bubbled through a toluene-d_8 solution of complex **3** for several minutes at room temperature and the ^1H NMR spectrum recorded. The spectrum generally showed broad, poorly resolved peaks. However, a major shift of the tolyl *o*-proton from 7.35 to 9.86 ppm was readily observed, providing evidence of CO insertion into the Ni–aryl bond. A similar shift was noted during the carbonylation of complex **1**. Studies by Fahey and Mahan have shown that for nickel benzoyl derivatives the resonances of *o*-protons are shifted markedly down-

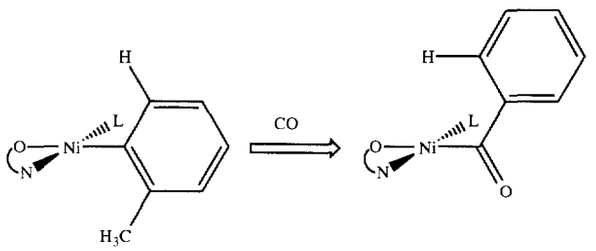

Fig. 3. *Ortho*-proton of *o*-tolyl ligand moving closer to the metal centre upon CO insertion into the M–C bond supported by previous observations [33].

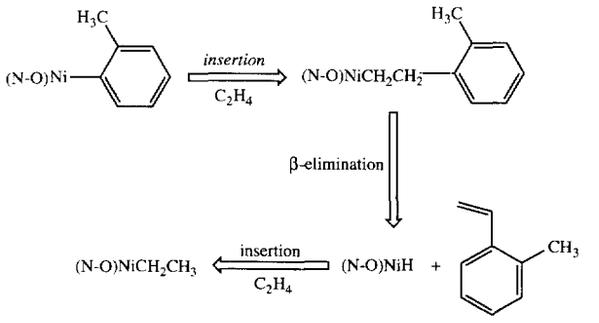

Fig. 4. Generation of the active Ni–H (Ni–alkyl) species for the complexes [Ni(*o*-tolyl)(X-pyca)PPh_3].

field (e.g. from 7.23 to 8.44 ppm); insertion of CO allows the *o*-proton to move closer to the metal centre, above or below the coordination plane of the complex (Fig. 3) [33]. Two new peaks due to tolyl–methyl protons (at 2.58 and 2.17 ppm), in addition to the peak from the original complex (at 2.61 ppm), were also observed.

3.3. Mechanistic considerations

The generally accepted mechanism for olefin polymerisation is that suggested by Cossee and Arlman [34]. This mechanism proposes that chain growth occurs through migratory insertion of substrate molecules into a metal–hydride (or metal–alkyl) bond. Termination of the growing chain is generally thought to occur via β-hydride elimination. In agreement with this mechanism, we noted the presence of the primary insertion product 2-methylstyrene. The observation of 2-methylstyrene is consistent with initial ethene insertion into the Ni–C bond followed by β-hydride elimination, generating a nickel hydride intermediate (Fig. 4) [35]. The nickel hydride rapidly inserts further ethene molecules leading to chain growth. Control of the molecular weight of the growing chain becomes a competition between the rate of insertion and the rate of β-hydride elimination (or chain transfer). Theoretical calculations [28] have indicated that the electron density on the nitrogen atom of the pyridyl ring for the free ligand is considerably reduced for 4-NO_2-pyca and pyzca compared to pyca and 4-MeO-pyca (Table 2). We note, therefore, that the reduction in basicity of the bidentate ligand appears to greatly facilitate the rate of migratory insertion compared with the rate of β-hydride elimination and therefore favours the production of polymeric rather than oligomeric products.

In a previous study [11], it was found that the addition of free phosphine ligand to Ni(*o*-tolyl)(pyca)PPh_3, during the catalytic conversion of ethene to higher oligomers, led to a relatively small drop in activity [0.5 equiv. excess PPh_3 approximately halved the activity and 1 equiv. excess PPh_3 led only to a 2/3 reduction in activity]. This observation, combined with the failure to detect any evidence of ligand dissociation or ligand exchange even when the complex was heated in the presence of excess PPh_3, suggested that

Table 4
Selected bond lengths (Å) and angles (°) for the complexes [Ni(*o*-tolyl)(4-NO_2-pyca)PPh_3] and [Ni(*o*-tolyl)(pyca)PPh_3], with data for [Ni(mes)(pyca)$PMePh_2$] [11] included for comparison

	[Ni(*o*-tolyl)(NO_2-pyca)PPh_3]	[Ni(*o*-tolyl)(pyca)PPh_3]	[Ni(mes)(pyca)$PMePh_2$]
Ni–P	2.163(2)	2.163(2)	2.148(2)
Ni–N(1)	1.940(4)	1.945(4)	1.926(6)
Ni–O(21)	1.931(3)	1.919(3)	1.911(5)
Ni–C(101)	1.851(7)	1.884(5)	1.865(8)
Ni–C(101′)	1.92(1)	—	
P–Ni–N(1)	176.3(1)	176.7(1)	176.6(2)
P–Ni–O(21)	92.4(1)	92.7(1)	92.1(2)
P–Ni–C(101)	90.9(2)	89.3(2)	89.7(2)
P–Ni–C(101′)	92.0(4)	—	—
N(1)–Ni–O(21)	84.0(1)	84.1(1)	84.6(2)
C(101)–Ni–O(21)	169.9(3)	173.7(2)	177.2(3)
C(101′)–Ni–O(21)	170.8(3)	—	—
C(101)–Ni–N(1)	92.7(3)	94.0(2)	93.6(3)
C(101′)–Ni–N(1)	91.6(4)	—	

Table 5
Non-hydrogen positional and isotropic displacement parameters for **1**

Atom	x	y	z	U_{eq} (Å^2)
Ni	0.27425(2)	0.40594(2)	0.34131(3)	0.0475(3)
P	0.28166(4)	0.47305(4)	0.39282(7)	0.0467(5)
C(11)	0.2557(2)	0.4737(1)	0.4964(3)	0.050(2)
C(12)	0.2745(2)	0.4661(2)	0.5713(3)	0.068(3)
C(13)	0.2535(2)	0.4647(2)	0.6492(3)	0.087(4)
C(14)	0.2125(2)	0.4701(2)	0.6545(3)	0.093(4)
C(15)	0.1936(2)	0.4770(3)	0.5813(4)	0.105(4)
C(16)	0.2146(2)	0.4786(2)	0.5025(3)	0.079(3)
C(21)	0.3459(1)	0.5206(2)	0.3991(3)	0.052(2)
C(22)	0.3635(2)	0.5585(2)	0.4579(3)	0.070(3)
C(23)	0.4124(2)	0.5955(2)	0.4541(4)	0.092(3)
C(24)	0.4427(2)	0.5948(2)	0.3925(4)	0.098(3)
C(25)	0.4255(2)	0.5577(2)	0.3344(4)	0.092(3)
C(26)	0.3773(2)	0.5206(2)	0.3384(3)	0.071(3)
C(31)	0.2547(2)	0.4991(2)	0.3223(3)	0.052(2)
C(32)	0.2748(2)	0.5483(2)	0.3076(3)	0.074(3)
C(33)	0.2506(2)	0.5654(2)	0.2551(4)	0.092(4)
C(34)	0.2064(2)	0.5327(2)	0.2182(3)	0.093(4)
C(35)	0.1864(2)	0.4838(2)	0.2326(3)	0.089(4)
C(36)	0.2102(2)	0.4670(2)	0.2832(3)	0.068(3)
N(1)	0.2667(1)	0.3466(1)	0.2886(2)	0.048(2)
C(2)	0.2664(1)	0.3489(1)	0.2035(3)	0.047(2)
C(201)	0.2724(2)	0.3964(2)	0.1688(3)	0.054(2)
O(21)	0.2767(1)	0.4272(1)	0.2258(2)	0.061(2)
O(22)	0.2715(1)	0.4019(1)	0.0913(2)	0.074(2)
C(3)	0.2616(2)	0.3111(2)	0.1516(3)	0.064(3)
C(4)	0.2570(2)	0.2697(2)	0.1890(3)	0.075(3)
C(5)	0.2569(2)	0.2663(2)	0.2757(3)	0.074(3)
C(6)	0.2618(2)	0.3055(2)	0.3235(3)	0.062(2)
C(101)	0.2787(2)	0.3861(2)	0.4528(3)	0.065(3)
C(102)	0.2388(2)	0.3554(2)	0.4992(3)	0.081(3)
C(1021)	0.1896(2)	0.3400(2)	0.4707(4)	0.099(3)
C(103)	0.2445(2)	0.3358(2)	0.5804(4)	0.098(4)
C(104)	0.2904(3)	0.3519(2)	0.6063(4)	0.111(4)
C(105)	0.3319(2)	0.3850(3)	0.5641(4)	0.116(5)
C(106)	0.3272(2)	0.4012(2)	0.4854(3)	0.081(3)
O(01) [a]	0.4930(5)	0.4601(5)	0.473(1)	0.23(1)
C(02) [a]	0.4651(6)	0.4554(6)	0.523(1)	0.17(1)
C(03) [a]	0.4885(6)	0.4793(8)	0.567(1)	0.24(2)
C(04) [a]	0.5317(8)	0.5186(9)	0.549(2)	0.26(2)
C(05) [a]	0.5318(8)	0.5027(9)	0.461(1)	0.24(2)
O(01′) [a]	0.307(2)	0.678(2)	0.648(3)	0.56(2)
C(02′) [a]	0.347(2)	0.687(2)	0.588(3)	0.56(2)
C(03′) [a]	0.327(3)	0.655(3)	0.519(3)	0.56(2)
C(04′) [a]	0.289(2)	0.606(2)	0.569(4)	0.56(2)
C(05′) [a]	0.271(2)	0.624(2)	0.645(4)	0.56(2)

[a] Site occupancy factors: O(01)–O(05) 0.5, O(01′)–O(05′) 1/3.

for nickel complexes containing non-substituted pyca ligands, the insertion reaction of the coordinated olefin may occur from a five-coordinate intermediate i.e. via an associative mechanism [11]. An alternative mechanism is the dissociative route in which insertion occurs from a four-coordinate intermediate, following ligand displacement. A propagation mechanism involving substitution of the monodentate phosphine ligand by ethene, forming a four-coordinate σ-alkyl, π-olefin complex, has been suggested for SHOP-type polymerisation systems [14].

A variable temperature ^{31}P NMR study of complex **3**, [Ni(*o*-tolyl)(4-NO_2-pyca)PPh_3], in the presence of excess phosphine, in contrast to the behaviour of com-

Table 6
Non-hydrogen positional and isotropic displacement parameters for **3**

Atom	x	y	z	U_{eq} (Å^2)
Ni	0.27257(2)	0.40473(2)	0.33469(3)	0.0501(3)
P	0.28235(4)	0.47096(4)	0.38726(7)	0.0462(6)
C(11)	0.2589(2)	0.4745(2)	0.4892(2)	0.048(2)
C(12)	0.2727(2)	0.4600(2)	0.5605(3)	0.062(3)
C(13)	0.2545(2)	0.4631(2)	0.6374(3)	0.079(3)
C(14)	0.2244(2)	0.4806(2)	0.6456(3)	0.089(4)
C(15)	0.2113(2)	0.4959(2)	0.5755(3)	0.092(4)
C(16)	0.2281(2)	0.4925(2)	0.4971(3)	0.072(3)
C(21)	0.3456(2)	0.5158(2)	0.3899(3)	0.053(2)
C(22)	0.3662(2)	0.5499(2)	0.4511(3)	0.083(3)
C(23)	0.4144(2)	0.5854(2)	0.4451(3)	0.105(4)
C(24)	0.4406(2)	0.5869(2)	0.3783(3)	0.100(3)
C(25)	0.4206(2)	0.5540(2)	0.3162(3)	0.093(3)
C(26)	0.3737(2)	0.5179(2)	0.3229(3)	0.072(3)
C(31)	0.2561(2)	0.4958(2)	0.3185(2)	0.054(3)
C(32)	0.2769(2)	0.5443(2)	0.3019(3)	0.075(3)
C(33)	0.2524(2)	0.5614(2)	0.2527(3)	0.099(4)
C(34)	0.2072(2)	0.5292(2)	0.2217(3)	0.102(4)
C(35)	0.1870(2)	0.4817(2)	0.2377(3)	0.095(4)
C(36)	0.2113(2)	0.4648(2)	0.2849(3)	0.075(3)
N(1)	0.2645(1)	0.3472(1)	0.2806(2)	0.051(2)
C(2)	0.2669(2)	0.3519(1)	0.1968(2)	0.050(2)
C(201)	0.2779(2)	0.4001(2)	0.1655(3)	0.058(2)
O(21)	0.2809(1)	0.4292(1)	0.2224(2)	0.065(2)
O(22)	0.2823(1)	0.4.077(1)	0.0900(2)	0.079(2)
C(3)	0.2602(2)	0.3151(2)	0.1443(3)	0.060(3)
C(4)	0.2505(2)	0.2725(2)	0.1807(3)	0.062(3)
N(4)	0.2434(2)	0.2325(1)	0.1263(2)	0.086(3)
O(41)	0.2312(2)	0.1942(1)	0.1582(2)	0.117(3)
O(42)	0.2466(2)	0.2390(1)	0.0523(2)	0.142(3)
C(5)	0.2483(2)	0.2666(2)	0.2649(3)	0.065(3)
C(6)	0.2544(2)	0.3043(2)	0.3134(2)	0.059(3)
C(101) [a]	0.2751(2)	0.3823(2)	0.4397(4)	0.051(4)
C(102) [a]	0.2335(3)	0.3531(3)	0.4829(4)	0.073(4)
C(1021) [a]	0.1858(3)	0.3426(3)	0.4601(5)	0.099(5)
C(103) [a]	0.2367(4)	0.3304(3)	0.5585(5)	0.124(8)
C(104) [a]	0.2778(5)	0.3352(3)	0.5838(5)	0.138(9)
C(105) [a]	0.3214(4)	0.3686(4)	0.5430(5)	0.123(9)
C(106) [a]	0.3177(3)	0.3892(3)	0.4715(4)	0.074(5)
C(101′) [a]	0.2542(4)	0.3728(4)	0.4408(7)	0.044(6)
C(102′) [a]	0.2873(4)	0.3679(4)	0.4906(8)	0.051(7)
C(1021′) [a]	0.3397(4)	0.3942(5)	0.4679(8)	0.065(8)
C(103′) [a]	0.2751(7)	0.3420(6)	0.5575(7)	0.09(1)
C(104′) [a]	0.2242(6)	0.3099(6)	0.577(1)	0.10(1)
C(105′) [a]	0.1897(5)	0.3167(6)	0.5336(9)	0.085(9)
C(106′) [a]	0.2085(4)	0.3471(5)	0.4614(8)	0.068(7)
O(01) [a]	0.4724(7)	0.4971(8)	0.484(1)	0.38(2)
C(02) [a]	0.511(1)	0.518(1)	0.422(1)	0.32(3)
C(03) [a]	0.5548(6)	0.5456(8)	0.459(1)	0.25(2)
C(04) [a]	0.5414(9)	0.5320(9)	0.542(1)	0.29(2)
C(05) [a]	0.487(1)	0.498(1)	0.556(2)	0.34(3)
O(01′) [a]	0.316(2)	0.684(2)	0.590(2)	0.62(2)
C(02′) [a]	0.354(2)	0.698(2)	0.525(3)	0.62(2)
C(03′) [a]	0.333(4)	0.668(3)	0.452(2)	0.62(2)
C(04′) [a]	0.300(3)	0.625(2)	0.490(3)	0.62(2)
C(05′) [a]	0.289(2)	0.635(2)	0.584(2)	0.62(2)

[a] Site occupancy factors: C(101)–C(106) 0.656(3), C(101′)–C(106′) 1 − 0.656(3), O(01)–C(05) 0.5, O(01′)–C(05′) 0.333.

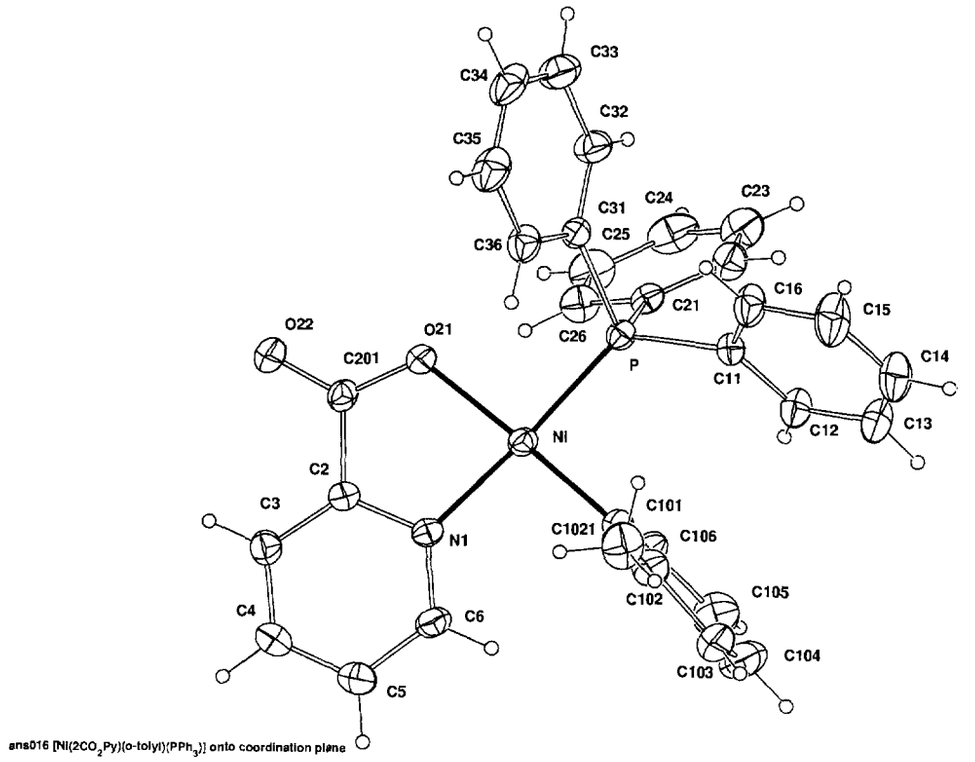

Fig. 5. Projection of the complex [Ni(*o*-tolyl)(pyca)PPh_3], **1**, normal to the coordination plane; 20% thermal ellipsoids are shown for the non-hydrogen atoms, hydrogen atoms having arbitrary radii of 0.1 Å.

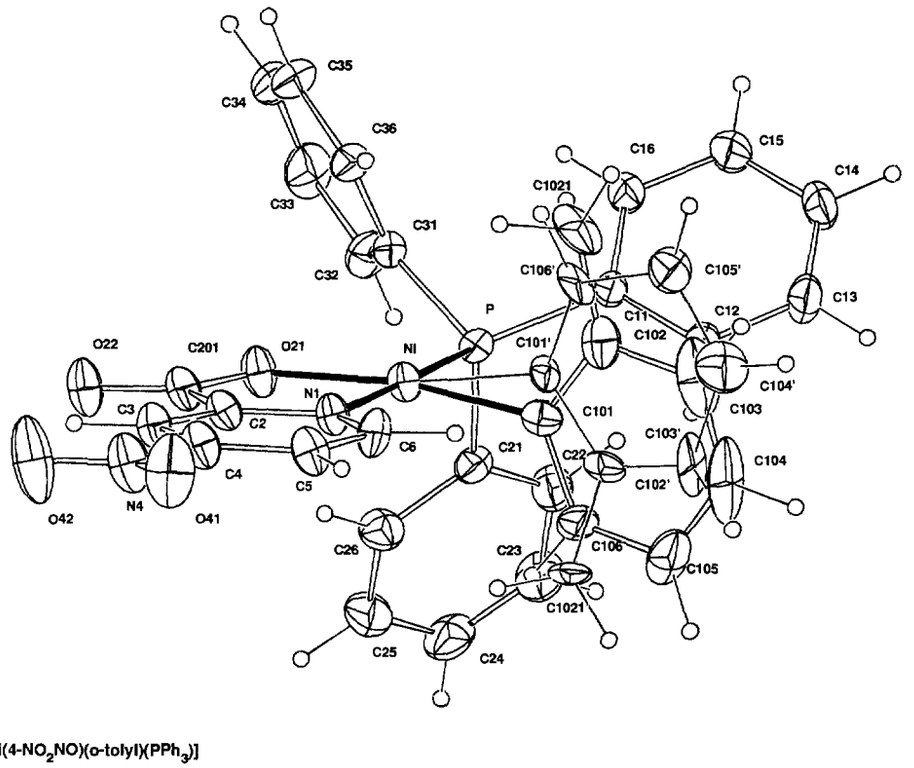

Fig. 6. Projection of the complex [Ni(*o*-tolyl)(NO_2-pyca)PPh_3], **3**, oblique to the coordination plane, showing the two disordered components of the *o*-tolyl group.

plexes containing non-substituted pyca [11], provided evidence of phosphine exchange. Furthermore, in the presence of ethene free phosphine was detected in solution at between 40 and 60 °C, which is consistent with ethene promoted ligand dissociation [8]. ^{1}H NMR at 80 °C showed extensive peak broadening and the *o*-tolyl *o*-H shifted upfield significantly (from 2.6 to 2.15 ppm). On the basis of this limited evidence, the possibility of two different pathways being followed (i.e. associative with non-substituted pyca ligand and dissociative with 4-substituted pyca ligand) may help explain the different products obtained with the two types of catalysts (i.e. oligomers with [Ni(*o*-tolyl)(pyca)PPh_3] **1** and polymers with [Ni(*o*-tolyl)(4-NO_2-pyca)PPh_3] **3**). Reduction in basicity of the substituted pyca ligand appears to greatly facilitate migratory insertion and therefore chain growth (by providing a facile dissociative route). As the basicity of the pyca ligand increases an associative insertion pathway involving a five-coordinate intermediate may be favoured producing shorter chain length products. Although chelate hemilability cannot be ruled out, NMR experiments favour phosphine dissociation. The expected weakening of the Ni–N bond caused by a reduction in electron density on the N is not supported by any changes in bond length between the complex [Ni(*o*-tolyl)(pyca)PPh_3] and the complex [Ni(*o*-tolyl)(4-NO_2-pyca)PPh_3] as shown by X-ray crystal structure data (vide infra).

Initiation of reaction in the case of ethene/carbon monoxide copolymerisation is achieved in the presence of ethene only. In the initial presence of CO in situ NMR experiments provided evidence for rapid decomposition of the complexes. However, following the generation of the active nickel hydride (or alkyl) catalyst, the addition of CO then initiates the polyketone chain growth. The copolymerisation of CO/C_2H_4 probably proceeds by sequential insertions of CO into the M–alkyl bond, and ethene into the M–acyl bond, as reported for several palladium based systems [15,36–43], including one palladium catalyst species containing a pyridine carboxylate chelate ligand [10]. Studies by Rix and Brookhart [44] have shown the M–acyl intermediate to be the resting state, restricting β-hydride elimination. This is supported by the absence of any detectable oligomeric keto products.

3.4. Crystal structures of the complexes [Ni(o-tolyl)(pyca)PPh_3] and [Ni(o-tolyl)(4-NO_2-pyca)PPh_3]

Selected bond distances and angles are provided in Table 4, together with comparative data for [Ni(mes)(pyca)($PMePh_2$)] [11]. Coordinates for the non-hydrogen atoms are given in Tables 5 and 6. Molecular projections of complexes **1** and **3** are shown in Figs. 5 and 6.

The complexes have the expected square planar

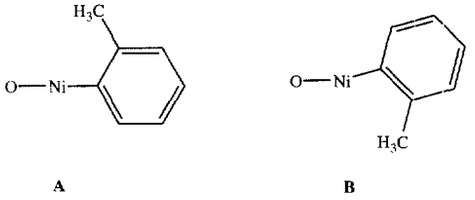

Fig. 7. View along the N–Ni–P axis of the two solid state conformers of complex [Ni(*o*-tolyl)(4-NO_2-pyca)PPh_3].

structure with phosphorus *trans* to the nitrogen of the pyca ligand and both crystallize in the rhombohedral space group $R\bar{3}$. Parameters relating to the coordination spheres around the nickel centre for the two complexes are very similar and it is apparent that the presence of the 4-NO_2 group has surprisingly little impact on the coordination structure. In particular the Ni–N bond [complex **1**, Ni–N = 1.945(4) Å; complex **3**, 1.940(4) Å] and the *trans* Ni–P bond [complex **1**, Ni–P = 2.163(2) Å; complex **3**, 2.163(2) Å] appear to be little affected by the introduction of the strongly electron withdrawing *p*-NO_2 group. The planes of the *o*-tolyl groups lie perpendicular to the NiCPNO plane. The dihedral angle for complex **1** is 85.2(2)° with the *o*-methyl group (C1021) above the plane minimising steric interactions between ligands; the NiPONC plane/C(101)–C(104) line dihedral angle is 82.5(1)°.

In complex **3** the *o*-tolyl ligand is disordered over two sites. The disorder is indicative of the presence in the solid state of two conformers, one where the methyl group of the *o*-tolyl ligand is above the NiCPNO plane (C1021) (Fig. 7, **A**) and the other where the *o*-methyl group is below the plane (C1021′) (Fig. 7, **B**). χ^2 for the NiPONC,C″ planes in **3** is 1193, 347 (for **1** it was 634) with deviation δ C(101,101′) respectively 0.218(7), —0.24(1) (0.134(7) Å in **1**). The dihedral angles of the C(101) C(104), C(101′) C(104′) lines to their respective planes are 82.5(1), 78.1(1)°. The dispositions of the two components are shown in Fig. 6. ^{1}H NMR indicates that only one conformer or an average of rapidly exchanging conformers is observed in solution, as indicated by the presence of a single sharp resonance for the *o*-Me protons. The Ni–C bond for conformer **B** [1.92(1) Å] may possibly be slightly longer than that for conformer **A** [1.851(7) Å], i.e. Ni C(101′) to Ni C(101) = 0.07(1) Å; their mean corresponds closely to the value found for the pyca complex, **1**.

4. Conclusions

For catalysts derived from arylnickel(II) complexes of the type [NiR(N–O)L], the presence of an electron withdrawing substituent in the 4-position of the pyridyl ring on the N–O chelate ligand transforms an oligomerisation catalyst into a polymerisation catalyst.

Complex **3**, [Ni(*o*-tolyl)(4-NO_2-pyca)PPh_3], is one of the few examples of a fully characterised organonickel(II) complex that has been reported to show catalytic CO/C_2H_4 copolymerisation activity. The performance of the nickel(II) complexes [NiR(N–O)L] for ethene polymerisation is strongly dependent on the basicity of the bidentate ligands. Although many aspects of the mechanism remain ambiguous, to explain the change in chain lengths of the products it is possible that catalysts derived from less basic, 4-substituted ligands may follow a different mechanistic pathway than that followed by catalysts derived from non-substituted ligand. In some examples both pathways may be operating concurrently.

Acknowledgements

We are indebted to the Australian Research Counsel for financial support and for providing an Australian Postgraduate Award for S.Y.D. We would also like to acknowledge Dr. Robert Brüll (RWTH, Aachen) for assisting S.Y.D. during the four months she spent working in Aachen. The assistance of Dr. Evan Peacock (CSL University of Tasmania) with the NMR experiments is also gratefully acknowledged.

References

[1] G.P.C.M. Dekker, A. Buijs, C.J. Elsevier, K. Vrieze, P.W.N.M. van Leewen, W.J.J. Smeets, A.L. Spek, Y.F. Wang, C.H. Stam, Organometallics 11 (1992) 1937.
[2] R.E. Rülke, J.G.P. Delis, A.M. Groot, C.J. Elsevier, P.W.N.M. van Leeuwen, K. Vrieze, K. Goubitz, H. Schenk, J. Organomet. Chem. 508 (1996) 109.
[3] R. van Asselt, E.E.C.G. Gielens, R.E. Rülke, K. Vrieze, C.J. Elsevier, J. Am. Chem. Soc. 116 (1994) 977.
[4] H. Jin, K.J. Cavell, B.W. Skelton, A.H. White, J. Chem. Soc., Dalton Trans. (1995) 2159.
[5] H. Jin, K.J. Cavell, J. Chem. Soc., Dalton Trans. (1994) 415.
[6] M. Brookhart, F.C. Rix, J.M. DeSimone, J. Am. Chem. Soc. 114 (1992) 5894.
[7] R. van Asselt, E.E.C.G. Gielens, R. Rülke, C.J. Elsevier, J. Chem. Soc., Chem. Commun. (1993) 1203.
[8] K.J. Cavell, H. Jin, J. Chem. Soc., Dalton Trans. (1995) 4081.
[9] J.L. Hoare, K.J. Cavell, R. Hecker, B.W. Skelton, A.H. White, J. Chem. Soc., Dalton Trans. (1996) 2197.
[10] M.J. Green, G.J.P. Britovsek, K.J. Cavell, B.W. Skelton, A.H. White, Chem. Commun. (1996) 1563.
[11] S.Y. Desjardins, K.J. Cavell, H. Jin, B.W. Skelton, A.H. White, J. Organomet. Chem. 515 (1996) 233.
[12] M. Brookhart, L.K. Johnson, C.M. Killian, S. Mecking, D.J. Tempel, Polymer Preprints (1996) 254.
[13] U. Klabunde, T.H. Tulip, D.C. Roe, S.D. Ittel, J. Organomet. Chem. 334 (1987) 141.
[14] U. Klabunde, R. Mulhaupt, T. Herskovitz, A.H. Janovicz, J. Calabrese, S.D. Ittel, J. Polym. Sci.: Polym. Chem. 25 (1987) 1989.
[15] U. Klabunde, S.D. Ittel, J. Molec. Catal. 41 (1987) 123.
[16] U. Klabunde, US Patents 4,698,403, 1987; 4,716,205, 1987; B. Driessen, M.J. Green, W. Keim, Eur. Pat. Appl. 470,759 A2, 1992; W. Keim, H. Maas, S. Mecking, Z. Naturforsch. 50b (1995) 430.
[17] D.F. Schriver, The Manipulation of Air Sensitive Compounds, McGraw-Hill, 1969.
[18] D.D. Perrin, W.L.F. Armarego, D.R. Perrin, Purification of Laboratory Chemicals, Pergamon Press, 1982.
[19] R.G. Hayter, F.S. Humiec, Inorg. Chem. 4 (1965) 1701.
[20] L.M. Venanzi, J. Chem. Soc. (1958) 719.
[21] S.R. Hall, H.D. Flack, J.M. Stewart (Eds.), The XTAL 3.2 Reference Manual, Universities of Western Australia, Geneva and Maryland, 1992.
[22] F. Krohnke, H. Schafer, Chem. Ber. 95 (1962) 1098.
[23] E. Matsumura, M. Ariga, T. Ohfuji, Bull. Chem. Soc. Jpn. 43 (10) (1970) 3210.
[24] E.V. Brown, M.B. Shambu, J. Org. Chem. 36 (14) (1971) 2002.
[25] S.B. Ford, Honours Thesis, University of Tasmania, Hobart, 1990.
[26] S. Desjardins, Honours Thesis, University of Tasmania, Hobart, 1991.
[27] A.R. Brause, M. Rycheck, M. Orchin, J. Am. Chem. Soc. 89 (1967) 6500.
[28] K. Frankcomb, B. Yates, K.J. Cavell, unpublished results, 1994.
[29] J.P. Collman, L.S. Hegedus, J.R. Norton, R.G. Finke, Principles and Applications of Organotransition Metal Chemistry, Mill Valley, CA, 2nd ed., 1987.
[30] J.S. Brumbaugh, R.R. Whittle, M. Parvez, A. Sen, Organometallics 9 (1990) 1735.
[31] P.E. Garrou, R.F. Heck, J. Am. Chem. Soc. 98 (1976) 4115.
[32] A. Sen, T.-W. Lai, J. Am. Chem. Soc. 104 (1982) 3520.
[33] D.R. Fahey, J.E. Mahan, J. Am. Chem. Soc. 99 (1976) 2501.
[34] P. Cossee, E.J. Arlman, J. Catal. 3 (1964) 99.
[35] W. Keim, A. Behr, B. Gruber, B. Hoffmann, F.H. Kowalt, U. Kürschner, B. Limbäcker, F.P. Sistig, Organometallics 5 (1986) 2356.
[36] E. Drent, J.A.M. van Broeckhoven, M.J. Doyle, J. Organomet. Chem. 417 (1991) 235.
[37] A.X. Zhao, J.C.W. Chien, J. Polym. Sci.: Polym. Chem. 30 (1992) 2735.
[38] B. Driessen-Hölsher, Dissertation, RWTH, Aachen, 1992.
[39] G.P.C.M. Dekker, A. Buijs, C.J. Elsevier, K. Vrieze, P.W.N.M. van Leewen, Organometallics 11 (1992) 1598.
[40] G.P.C.M. Dekker, C.J. Elsevier, K. Vrieze, P.W.N.M. van Leewen, C.F. Roobeck, J. Organomet. Chem. 430 (1992) 357.
[41] F. Ozawa, T. Hayashi, H. Koide, A. Yamamoto, J. Chem. Soc., Chem. Commun. (1991) 1469.
[42] W.M. Vetter, A. Sen, J. Organomet. Chem. 378 (1989) 485.
[43] T.-W. Lai, A. Sen, Organometallics 3 (1984) 866.
[44] F. Rix, M. Brookhart, J. Am. Chem. Soc. 117 (1995) 1137.